Investigation of Heat Transfer and Entropy Generation of Natural Convection in Gambrel Roof

Ogwumike, T.E, Olakoyejo, O.T*, Musah, A.A, Oloruntoba, O.T and Oyekeye, M.O

Department of Mechanical Engineering, University of Lagos, Akoka, Lagos, Nigeria

*Corresponding author's email: oolakoyejo@unilag.edu.ng

Abstract

A numerical study has been executed for a 2D laminar natural convection in Gambrel roof with boundary conditions that depict a hot weather climate in Nigeria. A commercial numerical code is used to model the design conditions. As a result of symmetry of the Gambrel roof geometry, half of the roof is used to carry out the study. The inclined roof and bottom roof surfaces are kept isothermally heated and cooled respectively, while the vertical surface at the symmetry line is kept adiabatic. Air is used as the coolant in this analysis. The effects of base (α) and top (ϕ) pitch angles and Rayleigh number (Ra) on the heat transfer and entropy generation characteristics are investigated. The results are presented by Nusselt number (Nu), entropy generation, isotherms and streamlines. Isotherms are seen to be smooth and uniform at lower Ra, while they undergo distortion at higher Ra. When the pitch angles are fixed, the effect of Ra on the Nu is not significant until $Ra > 10^5$, after which the relationship between Ra and Nu is becomes clearly linear. At fixed Ra, reducing α causes an increase in total entropy generation and Nu while increasing the ϕ causes a slight increase in the Nu. The physical implication of this is that at fixed Ra, the best convective heat transfer process is achieved by reducing α and increasing ϕ. This study would prove useful to designers in improving the thermal comfort of buildings with the Gambrel roof for a summer climate condition.

Keywords: *Natural convection, Pitch angle, Nusselt number, Entropy generation*

1. Introduction

Natural convection, by virtue of its low cost of maintenance and minimal noise emission, spans a wide array of engineering purposes such as cooling in heat exchangers, cooling of electronic equipment, solar collectors, nuclear reactors and even in the design of roofing structures. Climate condition influences the convective heat transfer that occurs within enclosures and roofing structures and the investigation of this convective transfer can prove useful in enhancing thermal comfort and energy efficiency.

Varol et al. (2007) focused their study solely on Gambrel roof type under summer and winter conditions and found out that Rayleigh number had a linear relationship with Nusselt number in both cases and that heat transfer in the roof is more enhanced in winter conditions compared to summer. Koca et al. (2007) studied the natural convective heat transfer within various roof type geometries under winter climate and observed that at small Rayleigh numbers, the smallest heat transfer occurred in Gambrel. Zhai et al. (2021) used direct numerical simulations to examine the natural convection occurring in a triangular shaped roof surface. Using air as the working fluid, they studied the flow as it transitioned from a steady state to a chaotic state. They observed various pitchfork bifurcations were in between various Rayleigh numbers and that the relationship between the flow and the Rayleigh number was directly proportional as weak flows occurred at low Rayleigh numbers while strong flows occurred as the Rayleigh number increased. A number of other similar studies on convective heat transfer have been carried out (Polo-Labarrios et al., 2020; Akinsete and Coleman, 1982; Shankar et al., 2018; Solomon and Kamiyo, 2020; Wang et al., 2021).

Production of irreversibilities during heat transfer results in energy loss in a system, and the measure of these irreversibilities can be evaluated

by monitoring the entropy generation rate. Hence, the investigation of entropy generation is important as heat transfer can be optimized by reducing entropy generation. Researches have been carried out on the entropy generation as a result of natural convection (Wei et al., 2017; Shavik et al., 2014; Zhang et al., 2021; Ziapour and Dehnavi, 2012; Ishak et al., 2021; Morsli et al., 2017).

Koca et al. (2007) carried out a similar study where they investigated natural convection in various roof types for winter condition only, one of which included the Gambrel roof and they studied the effect of pitch angle and Rayleigh number ranging from 10^3-10^6 with their results presented by Nusselt numbers, isotherms and streamlines. However, this study focuses on summer condition which indicates a hot weather climate, as can be seen in Nigeria and other African countries and goes further by employing the use of entropy generation to present the results of the investigation of natural convection in Gambrel roof with Rayleigh number ranging from 10^3-10^7.

2. Materials and methods

It is essential to define a physical model of the problem, before acquiring the solution to the various governing equations that are associated with the problem. The physical model of the Gambrel roof geometry is shown in Fig. 1. The model entails a 3D view of the roofing geometry, showing the boundary conditions governing the fluid flow within the structure.

By assumption, the model is later reduced to a 2D model. The study is aimed at analysing the natural convective heat transfer and entropy generation characteristic in the 2D structure. However, due to symmetry of the geometry of the Gambrel roof, only one half of the geometry is chosen as the computational domain as illustrated in Fig. 2a. The discretised computational domain is shown in Fig. 2b. It is considered that the inclined wall (roof) surfaces have constant hot temperature, T_H, and the bottom surface of the roof, which is the ceiling, has constant cold temperature, T_C, with $T_H > T_C$. The vertical wall surface is kept insulated. This configuration simulates a hot weather environment condition.
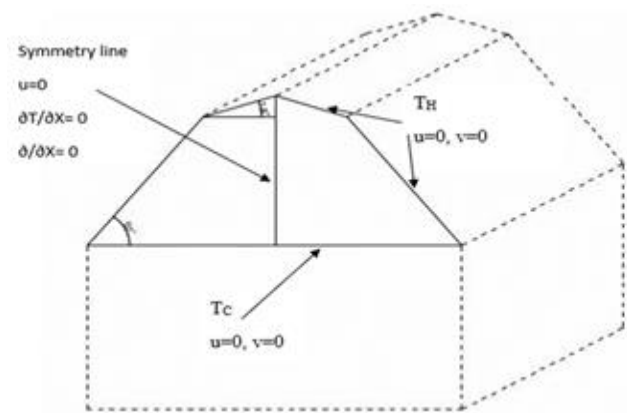

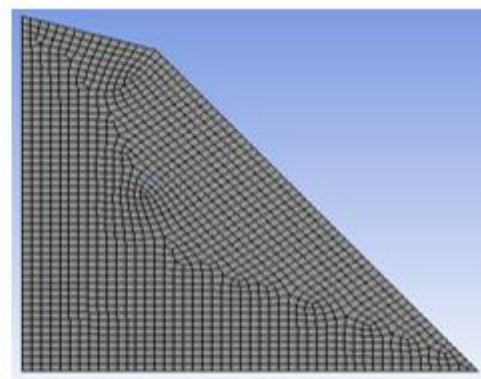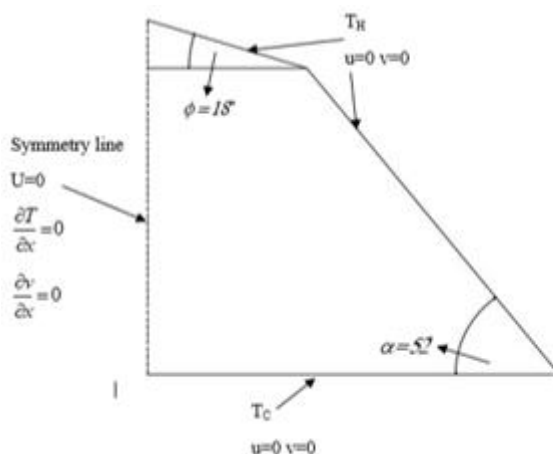**Fig. 1:** 3D schematic diagram of gambrel roof type (Koca et al., 2007)

Fig. 2: (a) 2D computational domain and (b) Mesh of computational domain of gambrel roof

The system is considered to be steady state and two-dimensional, having compressible laminar flow regime and Newtonian fluid. Thus, governing equations of mass, momentum and energy are expressed in Equations (1) – (4) as:

$$\frac{du}{dx} + \frac{dv}{dy} = 0 \tag{1}$$

$$\rho\left(u\frac{du}{dx} + v\frac{du}{dy}\right) = -\frac{dp}{dy} + \rho v \nabla^2 v \tag{2}$$

$$\rho\left(u\frac{du}{dx}+v\frac{du}{dy}\right)$$
$$=-\frac{dp}{dy}+\rho v\nabla^2 u$$
$$+\rho g\beta(T-T_\infty) \quad (3)$$

$$u\frac{dT}{dx}+v\frac{dT}{dy}=\alpha\nabla^2 T \quad (4)$$

where u and v are the x and y component of velocity, ρ the density, T the temperature, p the pressure, g the gravitational acceleration, μ the dynamic viscosity, ν the kinematic viscosity, α the thermal diffusivity and β the thermal expansion coefficient. Based on the governing equations, the non-dimensional variables are given as:

$$X=\frac{x}{h}, Y=\frac{y}{h}, U=\frac{uH}{\alpha}, V=\frac{vH}{\alpha},$$
$$\theta=\frac{T-T_C}{T_H-T_C}, P=\frac{pH^2}{\rho V^2}, Pr=\frac{v}{\alpha},$$
$$Ra=\frac{g\beta(T_H-T_C)H^3}{v\alpha} \quad (5)$$

Substituting all the dimensionless variables into the Equations (1) - (4) the dimensionless forms of the equations are expressed as:

$$\frac{dU}{dX}+\frac{dV}{dY}=0 \quad (6)$$

$$\left(\frac{Ra}{Pr}\right)^{\frac{1}{2}}\left(U\frac{dU}{dX}+V\frac{dV}{dY}\right)=-\frac{dP}{dX}+\nabla^2 U \quad (7)$$

$$\left(\frac{Ra}{Pr}\right)^{\frac{1}{2}}\left(U\frac{dU}{dX}+V\frac{dV}{dY}\right)=-\frac{dP}{dY}+\nabla^2 V+\left(\frac{Ra}{Pr}\right)^{\frac{1}{2}}\theta$$
$$(8)$$

$$\left(Ra\,Pr\right)^{\frac{1}{2}}\left(U\frac{d\theta}{dX}+V\frac{d\theta}{dY}\right)=\nabla^2\theta \quad (9)$$

where U and V are the X and Y component of dimensionless velocity, P the dimensionless Pressure, Ra the Rayleigh number, Pr the Prandtl number and θ the Dimensionless temperature.

The dimensionless thermal and frictional entropy generation due to irreversibility are expressed in Equations (10) and (11) respectively as:

$$S_{thermal}=\left[\left(\frac{d\theta}{dX}\right)^2+\left(\frac{d\theta}{dY}\right)^2\right] \quad (10)$$

$$S_{friction}=N_\mu\left[2\left[\left(\frac{dU}{dX}\right)^2+\left(\frac{dV}{dY}\right)^2\right]\right.$$
$$\left.+\left(\frac{\partial^2 U}{\partial Y^2}+\frac{\partial^2 V}{\partial X^2}\right)^2\right] \quad (11)$$

where N_μ is the irreversibility distribution ratio, given by:

$$N_\mu=\frac{\mu T_o}{K}\left(\frac{\alpha}{L(\Delta T)}\right)^2 \quad (12)$$

Therefore, total entropy generation is expressed as:

$$S_{Total}=S_{thermal}+S_{friction} \quad (13)$$

The boundary conditions in dimensionless form are given as:

1. Wall bottom T_C, $U=V=\theta=0$

2. Wall inclined T_H, $\theta=1; U=V=0$

3. Wall symmetry $U=\frac{dT}{dX}=\frac{dV}{dX}=0$

4. Wall vertical (Insulated), $q''=U=V=\frac{dT}{dX}=0$

ANSYS FLUENT based on finite volume method (FVM) was employed in solving the governing equations and imposed boundary conditions (Patankar and Spalding, 1972). The schematic diagrams for the various roof geometries were constructed using ANSYS FLUENT geometry design modeller in 2D format after which the meshing application on the ANSYS FLUENT software was used to generate the appropriate mesh by creating named selections which specified the various boundary conditions at the different surfaces of the geometries. The semi-implicit method for pressure linked equations (SIMPLE) scheme algorithm was applied for the pressure-velocity coupling. A second-order upwind scheme was used to discretise the combined convection and diffusion terms in the momentum and energy equations. In the ANSYS FLUENT solution setup application, the fluid flow was set to steady state while the heat transfer within the various geometries was simulated by initiating the energy equation model. Within the solution setup application, the required materials, alongside the appropriate working fluid properties were defined. Once completed, the solution setup was initialized and then the run calculation command was actualized. The solution is believed to have converged when the normalized residuals of the

mass and momentum equations fall under 10^{-10} and while the residual convergence of the energy equation was set to less than 10^{-18}. A graphical display of the residual converged solution was shown simultaneously as the calculation was being ran. The results from this simulation were displayed in isotherms and streamlines which showed the temperature distribution across the entire surface of the various geometries and the total heat transfer rate across the various geometries were gotten.

A grid dependency test was carried out in order to ensure the accuracy of the numerical result. The convergence criteria are expressed in Equation (14). Table 1 shows the grid dependency test for top pitch angle, $\phi = 18^0$, base pitch angle, $\alpha = 52^0$ and $Ra = 10^3$. From the results, it was deduced that the most suitable mesh used was the 18163 cells density.

$$\left| \frac{Nu_i - Nu_{i-1}}{Nu_i} \right| \leq 0.01 \qquad (14)$$

Table 1: Grid dependency test table

Number of Cells	Nu	$\dfrac{\left| Nu_i - Nu_{i\text{-}1} \right|}{\left| Nu_i \right|}$
14215	24.3110	-
16112	24.5086	0.0081
18163	24.7537	0.0099
20893	24.9754	0.0089

The numerical code is validated by comparing the current study with the results obtained from Gambrel roof geometry of Koca et al. (2007) as shown in Figure 3. The results reveal similar pattern and error deviation of less than 28%.
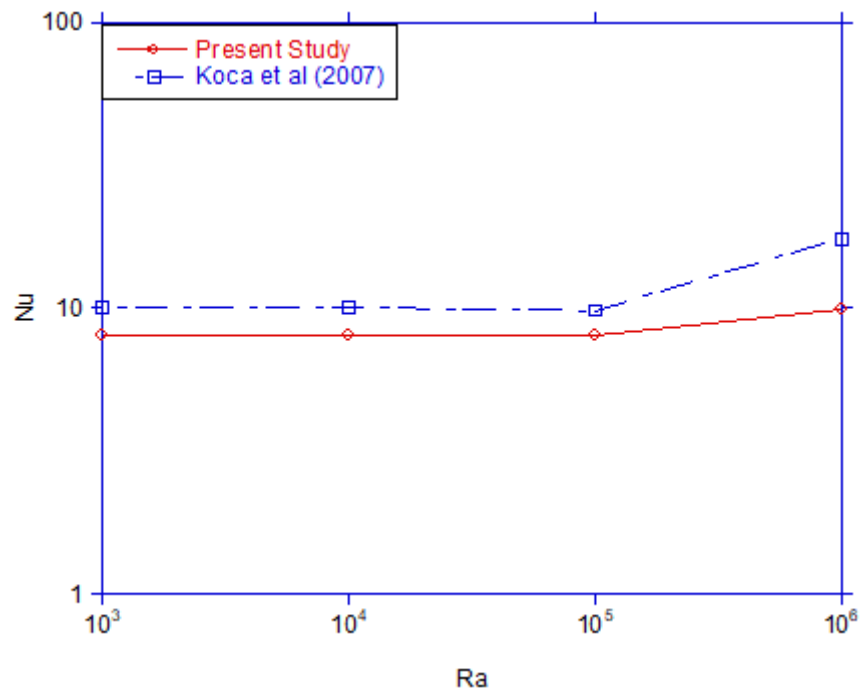

Fig 3: Comparison of the present study with Koca et al (2007)

3. Results and discussion

The results of the heat transfer analysis in terms of the influence of pitch and base angles and Rayleigh number on Nusselt number and entropy generation rate are presented here. Fig. 4 - 5 show the plot for fixed $Ra = 10^3$ while $\alpha = 48^0 - 56^0$ and $\phi = 12^0 - 20^0$. It shows that as α decreases, Nu increases while Nu experiences little or no change as ϕ is increased. The physical implication of this is that, in order to achieve the best convective heat transfer in Gambrel, α should be lowered. This would help in improving the thermal comfort in a

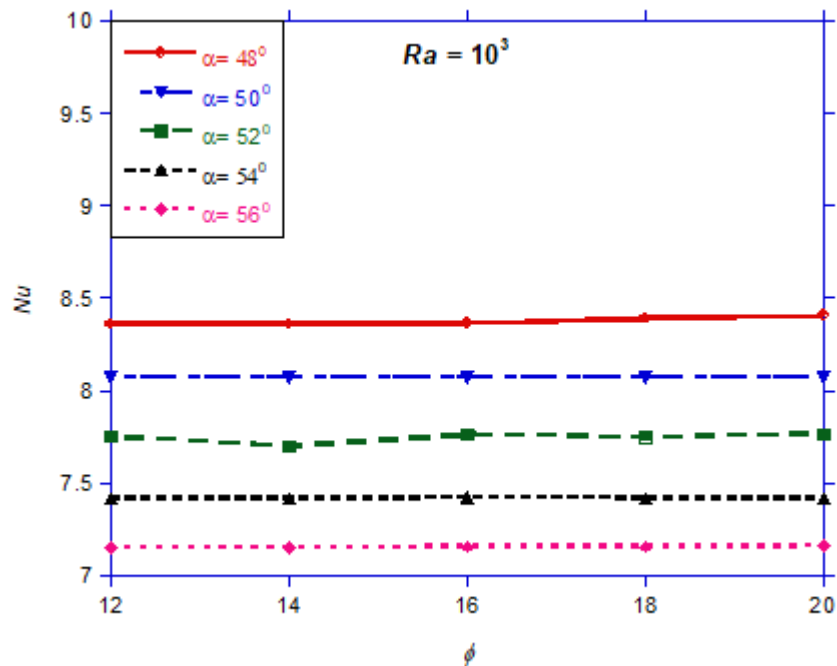building with the Gambrel roof type as improved heat transfer in the roof enhances the thermal comfort of the building.

Fig. 4: ϕ vs *Nu* at fixed Ra=10^3 and different α
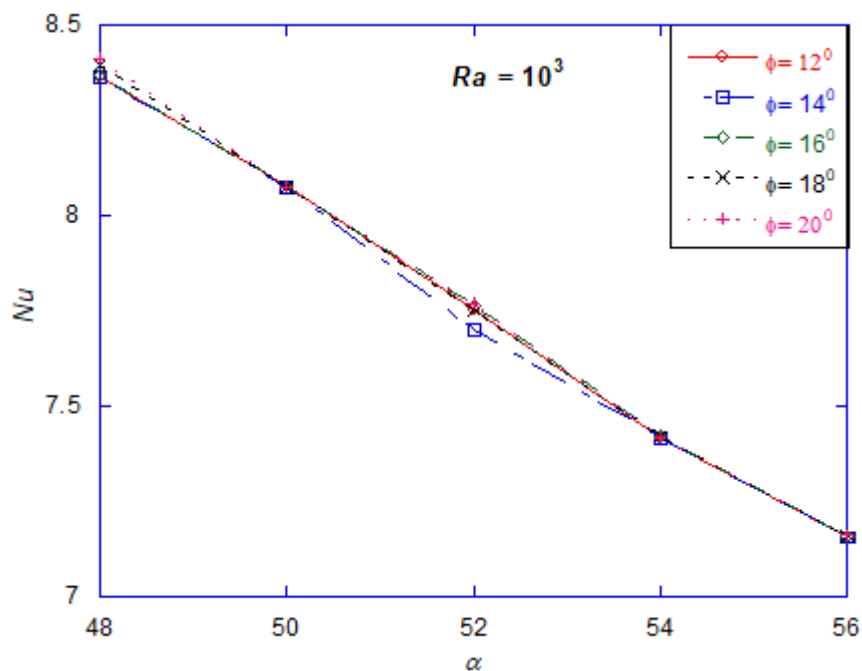
Fig. 5: α against *Nu* at fixed *Ra* =10^3 and different ϕ

Fig. 6 - 7 show the effect of *Ra* at different α and ϕ on *Nu*. It is observed that *Nu* increases as α decreases and ϕ increases. At lower Ra (Ra≤10^5), since conduction is the major mode of heat transfer, Nu is not responsive to Ra, but at higher Ra (Ra>10^5), Nu sharply increases in both cases, as fluid in the structure becomes strongly disturbed by convection mechanism. This shows that at the lower Rayleigh numbers (Ra=10^1-10^5), conduction mechanism dominates the heat transfer effect, and this is a result of weak buoyancy forces, which results in lower Nu values. However, at higher Rayleigh numbers (Ra=10^7), the buoyancy effect becomes evident and convection mechanism dominates the heat transfer, which results in an

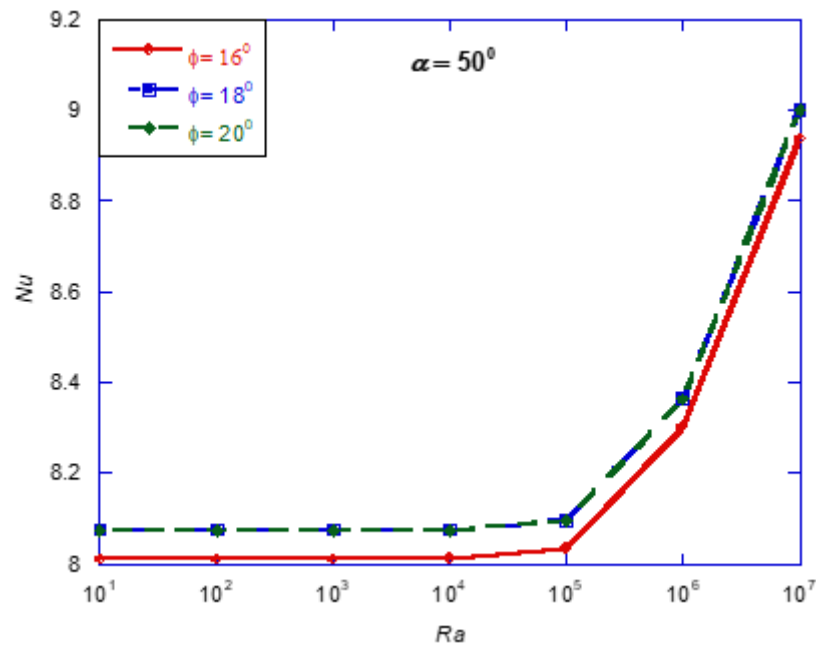increase in Nusselt number. This suggests improved thermal comfort may be achieved at higher Rayleigh numbers.

Fig. 6: *Ra* against Nu at different ϕ at fixed $\alpha = 50^0$ and different ϕ
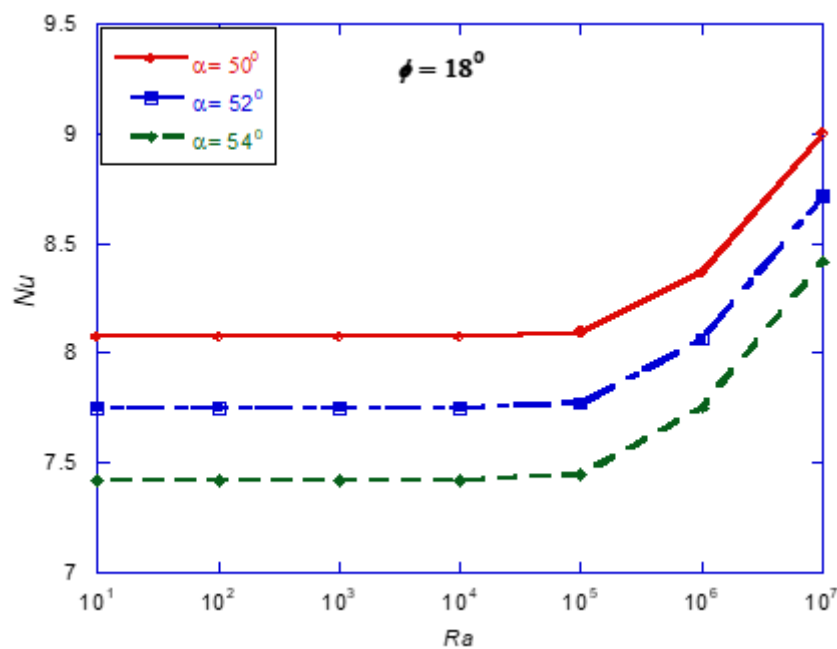

Fig. 7: *Ra* against *Nu* at different α and fixed $\phi = 18^0$

Fig. 8 - 9 show the effect of α on the various entropy generation at fixed Ra = 10^5 and different ϕ. It is observed that increasing α causes an increase in $S_{friction}$, and a decrease in $S_{thermal}$. This explains the opposite patterns that are seen in Fig. 8 with $S_{thermal}$ displaying a negative slope line while $S_{friction}$ displays a positive slope line. Since the entropy generation is dominated by $S_{thermal}$,

increasing α subsequently causes a decrease in S_{Total}. Hence Fig. 9 showcases a plot that is similar to trend displayed by $S_{thermal}$ in Fig. 8. Energy losses in a system causes entropy generation, hence, it is desirable to reduce the entropy generation. It implies that the energy losses in Gambrel can be minimized by increasing α.
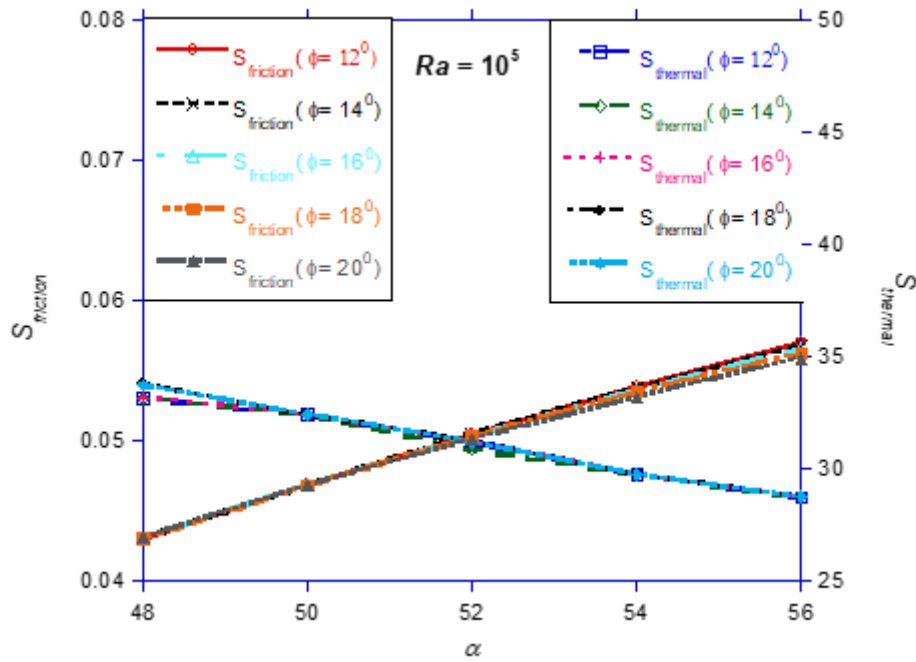
Fig. 8: α against $S_{thermal}$ and $S_{friction}$ at different ϕ at fixed Ra=10^5
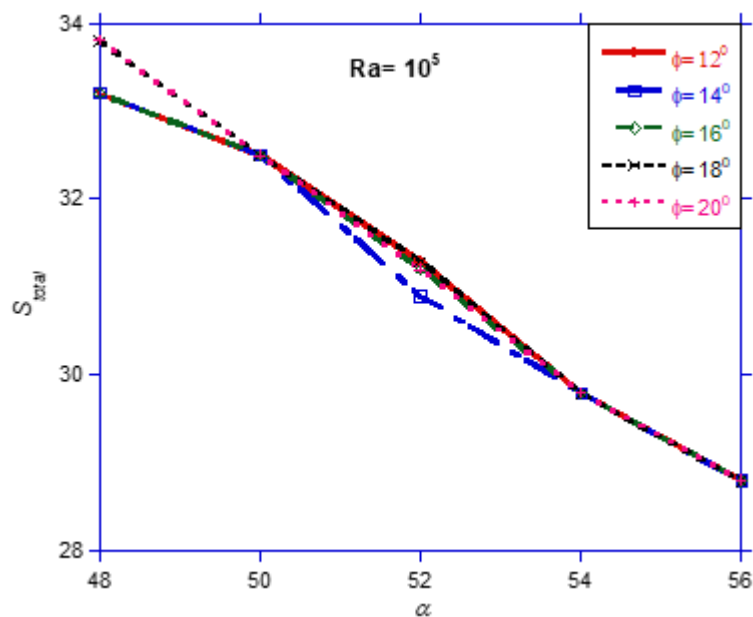

Fig. 9: α against S_{Total} at different ϕ at fixed Ra=10^5

Fig. 10 - 12 reveal the effect of Ra on $S_{thermal}$, $S_{friction}$ and S_{Total}, at fixed $\phi = 18^0$ and different α. It is observed that as Ra increases, $S_{thermal}$ and S_{Total} remain fairly constant until $Ra = 10^4$, after which $S_{thermal}$ and S_{Total} sharply increase. The effect of the Ra on $S_{friction}$ is insignificant until after the $Ra = 10^3$, after which $S_{friction}$ increases. Also, $S_{thermal}$ and S_{Total} decrease while $S_{friction}$ increases as α increases. Increasing Ra causes S_{Total} to rise due to increased heat transfer losses as the Ra rises, which affects the entropy generation by causing an increase in irreversibilities. This agrees with Hussein et al. (2016).

Fig. 13 shows the isotherms and streamlines at $Ra = 10^3 - 10^7$. It is observed that at lower $Ra = 10^3$ and 10^5, the flow pattern is observed to be one cell with lower magnitudes and the isotherms are uniformly distributed over the domain, which signifies that conduction is the

important heat transfer mode at this stage. But at higher $Ra = 10^7$, the magnitude is seen to intensify and the isotherm field undergoes significant distortion, as a result of the buoyancy induced convection flow within the Gambrel geometry at this stage.
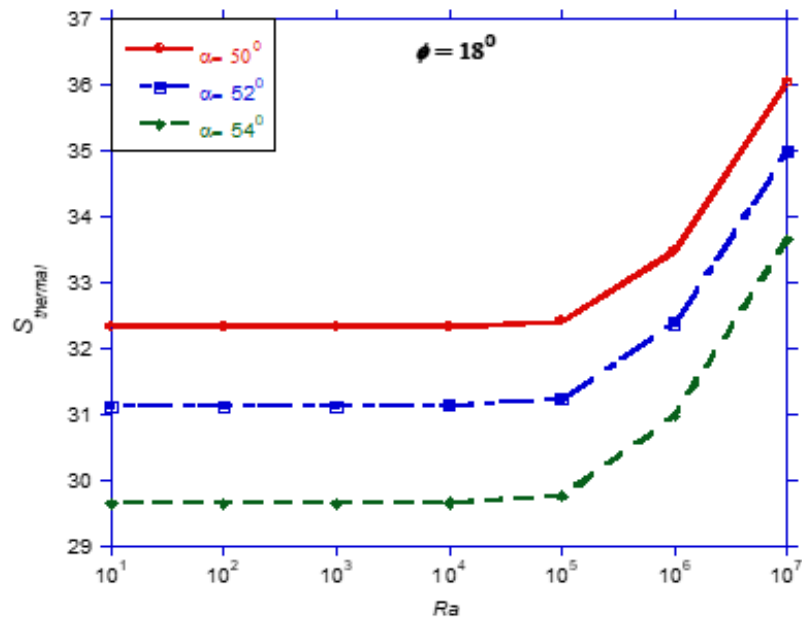

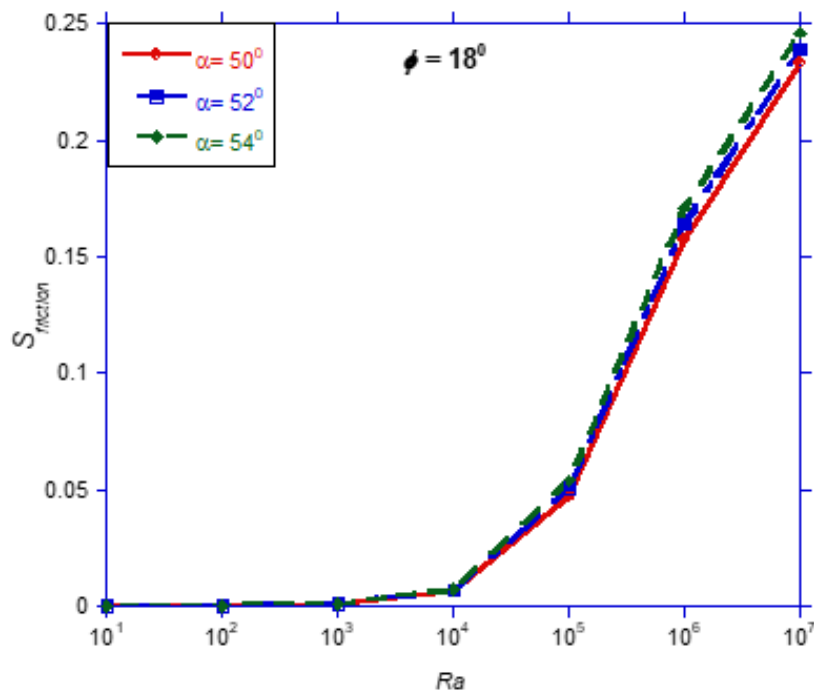**Fig. 10:** Ra against $S_{thermal}$ at fixed $\phi = 18^0$ and different α

Fig. 11: Ra against $S_{friction}$ at fixed $\phi = 18^0$ and different α
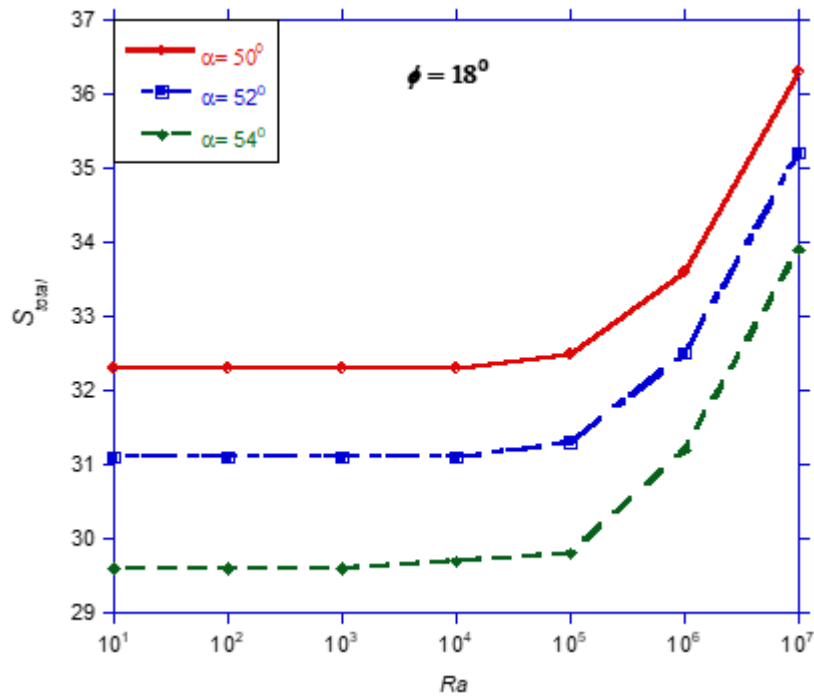
Fig. 12: Ra against S_{Total} at fixed $\phi = 18^0$ and different α
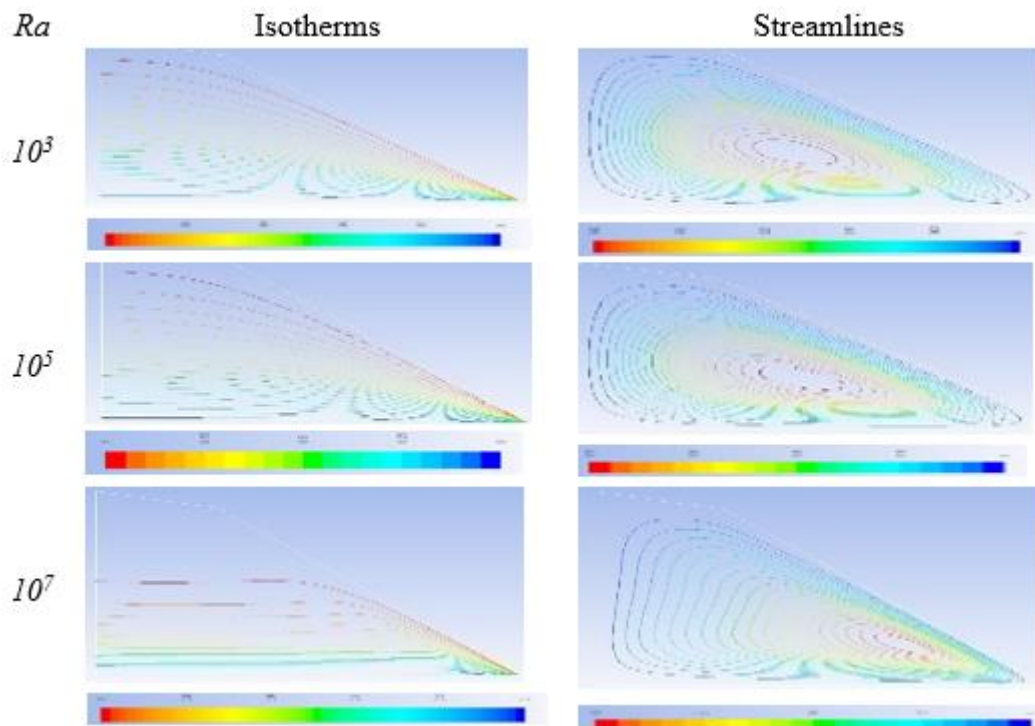

Fig. 13: Contour of isotherms and streamlines at different *Ra* at $\phi = 52^0$

4. Conclusion

A numerical study has been carried out for the 2D laminar natural convection in Gambrel roof type under hot weather conditions in Nigeria. The effect of pitch angles and Rayleigh number on heat transfer and entropy generation is analysed. It is observed that when α is fixed, increasing ϕ causes little or no change in *Nu*. When ϕ is fixed and α is varied, Nu increases as Ra increases. Similarly, when α is fixed and ϕ is varied, the

relationship between Nu and Ra is seen to be linear as Ra increases with an increase in Nu. However, the effect of Ra on Nu is not significant until $Ra > 10^5$ in both cases. The $S_{thermal}$ is dominated by $S_{thermal}$. At fixed Ra, decreasing α increases Nu and $S_{thermal}$ while $S_{friction}$ reduces. Since total entropy generation is dominated by $S_{thermal}$, reducing α also increases S_{Total}. When ϕ is kept constant, as α is decreased, increasing Ra results in an increase in S_{Total} and $S_{thermal}$. However, when ϕ is kept constant, increasing Ra increases $S_{friction}$ as α is increased. From streamlines and isotherms, at lower values of $Ra = 10^3 - 10^5$, the flow pattern is observed to be one cell with lower magnitudes with uniform isotherms but the magnitude intensifies and the isotherms become distorted at higher $Ra = 10^7$.

Acknowledgement

References

Akinsete, V.A. and Coleman, T.A. (1982) Heat transfer by steady laminar free convection in triangular enclosures. International Journal of Heat and Mass Transfer, 25(7): 991-998.

Ishak, M.S., Alsabery, A.I., Hashim, I. and Chamkha, A.J. (2021) Entropy production and mixed convection within trapezoidal cavity having nanofluids and localised solid cylinder. Scientific reports, 11(1): 1-22.

Koca, A., Oztop, H.F. and Varol, Y. (2007) Effects of Geometrical Shape of Roofs on Natural Convection for Winter Conditions. Proceedings of Clima WellBeing Indoors.

Morsli, S., Sabeur, A. and El Ganaoui, M. (2017) Influence of aspect ratio on the natural convection and entropy generation in rectangular cavities with wavy-wall. Energy Procedia, 139: 29-36.

Patankar, S.V. and Spalding, D.B. (1972) A calculation procedure for heat, mass and momentum transfer in three dimensional parabolic flows. International Journal of Heat and Mass Transfer, 15, 1787–1806.

Polo-Labarrios, M.A., Quezada-García, S., Sánchez-Mora, H., Escobedo-Izquierdo, M.A. and Espinosa-Paredes, G. (2020) Comparison of thermal performance between green roofs and conventional roofs. Case Studies in Thermal Engineering, 21, 100697.

Shankar, V., Bengston, A., Fransson, V. and Hagentoft, C.E. (2018) Numerical analysis of the influence of natural convection in attics–A CFD analysis. In AIP Conference Proceedings (Vol. 1978, No. 1, p. 470010). AIP Publishing LLC.

Shavik, S.M., Hassan, M.N., Morshed, A.M. and Islam, M.Q. (2014) Natural convection and entropy generation in a square inclined cavity with differentially heated vertical walls. Procedia Engineering, 90: 557-562.

Solomon, E. and Kamiyo, O. (2020) Natural Convection and Flow Simulation in Right-Angled Triangular Rooftop Enclosure under Winter Condition. International Organization of Scientific Research, 17(2): 07-15.

Varol, Y., Koca, A. and Oztop, H.F. (2007) Natural convection heat transfer in Gambrel roofs. Building and Environment, 42(3): 1291-1297.

Wang, Q., Li, J.E.R., Ren, Y., Li, J., Li, J. and Ma, M. (2021) Comparison study of natural convection between rectangular and triangular enclosures. AIP Advances, 11(4), 045303.

Wei, Y., Wang, Z. and Qian, Y. (2017) A numerical study on entropy generation in two-dimensional Rayleigh-Bénard convection at different Prandtl number. Entropy, 19(9), 443.

Zhai, H., Torres, J.F., Zhao, Y. and Xu, F. (2021) Transition from steady to chaotic flow of natural convection on a section-triangular roof. Physical Review Fluids, 6(1), 013502.

Zhang, X.H., Saeed, T., Algehyne, E.A., El Shorbagy, M.A., El-Refaey, A.M. and Ibrahim, M. (2021) Effect of L-shaped heat source and magnetic field on heat transfer and irreversibilities in nanofluid-filled oblique complex enclosure. Scientific Reports, 11(1): 1-19.

Ziapour, B.M. and Dehnavi, R. (2012) A numerical study of the arc-roof and the one-sided roof enclosures based on the entropy generation minimization. Computers & Mathematics with Applications, 64(6): 1636-1648.